# 16-th ECMI Modelling Week
# Final Report

23.08.2002—01.09.2002
Kaiserslautern, Germany

# Group 1

# Temperature Stabilisation during the Casting Process

**Christopher Halse**
*Department of Engineering Mathematics, University of Bristol, University Walk, Bristol, BS8 1TR, UK.*
**Vegard Kippe**
*Department of Mathematics, University of Trondheim, N-7034 Trondheim, Norway.*
**Alexander Pönitz**
*Institute of Computational Mathematics, University of Linz, Altenberger Straße 69, A-4040 Linz, Austria.*
**Benjamin Seibold**
*Department of Mathematics, University of Kaiserslautern, Postbox 3049, D-67653 Kaiserslautern, Germany.*

**Instructor: Prof. Dr. Wojciech Okrasiński**
*Institute of Mathematics, University of Zielona Góra, Poland.*

**Abstract**

This report considers the problem of stabilising the temperature in the mould during a casting process. A general mathematical model of the problem is formulated, as well as specific models. A simplified model disregarding the state transition between liquid and solid is solved in one and two dimensions. The 1D problem is solved by a Fourier coefficient method as well as a finite difference method. The Fourier method is also used to obtain certain results very inexpensively. The 2D problem is solved by fine elements using FEMLAB. The 1D finite difference method is then extended to a 1D model including the change of state, which requires to solve a problem with a moving boundary.

## 1.1 Introduction

For successful casting of certain AlSi parts (covers for electric devices) it is necessary that the mould has a sufficiently high temperature. If the temperature of the mould is too low the alloy cools too quickly, resulting in low quality parts. However, the required temperature is quite high, more than 300°C, meaning that both reaching and maintaining this temperature is problematic.
To maintain a high temperature the mould has 10-12 mm wide channels drilled into it, through which a 400°C liquid is pumped at a high velocity. Currently the required temperature is reached by performing the casting process and throwing away the low quality parts.
The casting process can be described as follows (Figure 1.1):

- Liquid alloy at a temperature of about 700°C is poured into the mould. ($\approx$ 3 seconds).
- The alloy is cooling and solidifying. ($\approx$ 60 seconds).
- The product is removed from the mould. ($\approx$ 15 seconds).
- The mould is closed and the process restarts.

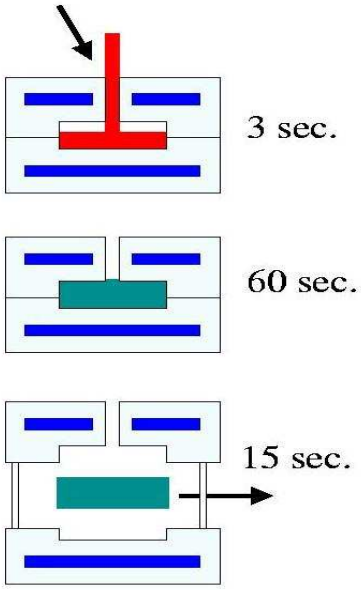


Figure 1.1: The casting process.

The temperature of the mould will rise gradually, and eventually production of high-quality parts can begin. From experience it is known that a stable

production temperature is reached after 60-80 iterations of the casting process. The cost of the products that have to be thrown away is negligible, more important is the time aspect. Currently it takes more than an hour to reach a stable temperature, and it is therefore of interest to investigate how to minimise this time. Of particular interest is the effect of the position of the channels and the influence of preheating the mould before casting starts. In Section 1.2 we will describe the important physical effects and derive the governing equations. We will set up one-dimensional and two-dimensional models, with different phenomena included respectively neglected. In Section 1.3 a Fourier method will be described, how the solution to the one-dimensional problem can be obtained directly. Section 1.4 will describe a finite difference approach for the same problem. In Section 1.5 the two-dimensional problem will be treated using FEMLAB. Section 1.6 will introduce the aspect of a moving boundary between liquid and solid alloy into the one-dimensional problem. In Section 1.7 the results will be summarised, and an outlook about how to continue our work will be given.

## 1.2 Basic Modelling

To minimise the stabilisation time a mathematical model of the heat transfer in the mould is desirable. The governing principle for this problem is conservation of heat. Denoting heat by $Q$ and the heat flux by $q$, the conservation law takes the following form in the absence of heat sources/sinks:

$$\frac{d}{dt}\int_{\Omega} Q \; dV + \int_{\partial\Omega} q \; dA = 0. \tag{1.1}$$

According to *Fourier's Law* the heat flux can be expressed as

$$q = -\kappa \nabla u, \tag{1.2}$$

where u is the temperature and $\kappa$ is the thermal conductivity, an experimentally determined constant. Also, by introducing the specific heat capacity $C_p$ and the density $\rho$, the heat can be written as $Q = \rho \cdot C_p \cdot u$. Inserting this into the conservation law and applying the divergence theorem gives,

$$\frac{d}{dt}\int_{\Omega} \rho \cdot C_p \cdot u \; dV + \int_{\Omega} \nabla q \; dV = 0. \tag{1.3}$$

The integration is over a constant volume so the differentiation can be moved inside, and the differential form of the conservation law is obtained by observing that the above equation must hold for subsets of the domain $\Omega$. After rearranging terms the differential form becomes:

$$u_t = D\nabla^2 u, \tag{1.4}$$

where the new constant, named the diffusivity or the diffusion constant, is defined as $D = \frac{\kappa}{\rho \cdot C_p}$.

## Models and Boundary Conditions

To apply equation (1.4) to the current problem the boundary conditions must be defined, which requires a closer look at the geometry and determination of the thermal properties of the different items involved.
The mould and the machinery has in reality a somewhat complicated geometry, but to obtain qualitative behaviour we consider a simplified geometry, where the machinery, the mould and the mould chamber are all cubic. The channels are also taken to have square cross sections[1], so that a vertical cross section of the mould will appear as shown in Figure 1.2.

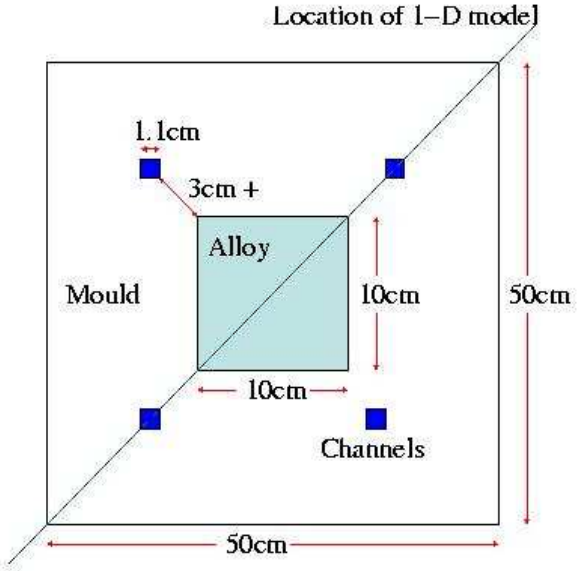


Figure 1.2: 2D cross section of the mould. The 1D model is taken to be along the diagonal.

The mould has a length of approximately 50 cm, while the mould chamber is approximately 10 cm long. The surrounding machinery is not shown in the figure, but has a size of about 150 cm. Because the mould is subjected to a high pressure during the cooling process, the minimum channel distance from the chamber is given to be 3 cm, and the size of the channels is about 11 mm. The cross section corresponds to a 2D model of the problem, while a 1D model is obtained by considering the diagonal as shown in the figure. A summary of the thermal properties of the mould and the alloy is shown in Table 1.1. The fact that the alloy changes state from liquid to solid will be ignored for the moment, and the properties given in the table are for solid alloy. (The state transition of the alloy will be considered in Section 1.6.)

[1] Actually the channels are drilled into the mould, meaning that they will have a circular cross section.

The surrounding machinery has properties very similar to the mould, hence they will be assumed equal.

| | $\kappa$ [W/Km] | $\rho$ [kg/m$^3$] | $C_p$ [J/kg K] | $D$ [m$^2$/s] |
|---|---|---|---|---|
| Mould | 30 | 7800 | 460 | $8.36 \cdot 10^{-6}$ |
| Alloy | 230 | 2650 | 920 | $94.34 \cdot 10^{-6}$ |

Table 1.1: Thermal properties

Obviously the conductivity of the mould is much less than the conductivity of the alloy, which partly explains why the temperature stabilisation process is so slow. Mathematically the conductivity difference is handled through the boundary conditions.
Considering the solution of equation (1.4) in the domain shown in Figure 1.2 it is evident that the temperature $u$ must be continuous across the alloy/mould border at all times, except at the exact moment when alloy is being poured into the mould chamber. The second boundary condition follows from applying the conservation principle at the boundary. Naming the alloy/mould boundary $\Gamma_M$ and applying Fourier's Law (1.2) on each side gives the flux continuity condition:

$$\kappa_1 \nabla u\big|_{\Gamma_M^+} = \kappa_2 \nabla u\big|_{\Gamma_M^-}, \tag{1.5}$$

where the index 1 refers to the mould and the index 2 refers to the alloy.
Naturally there will also be boundary conditions at the channel/mould and machine/air interfaces[2], but these pose no problem as they are simply of the Dirichlet type. While the channel/mould condition should be out of discussion, there are different possible boundary conditions how to model the heat loss from the machine to the air. Mostly precise would be *Newton's Law of Cooling*, but due to the low conductivity of the mould/machine the machine edges will not heat up significantly over the relevant timespan considered here, so it is sufficiently precise to prescribe Dirichlet boundary conditions of room temperature at the machine edges.
The resulting 1D and 2D models with boundary conditions are shown in Figure 1.2 (a) and (b). Note that the distance from the channels to the machine/air interface is greatly downscaled in Figure 1.2 (b).

### The Process of Repeated Casting

The initial condition when the casting starts is that the mould and machinery have room temperature ($\approx 30$°C), while the liquid alloy in the mould chamber is at 700°C. To obtain a time-continuous solution for the casting process the opening of the mould would have to be modelled. However, the

[2]There will be no mould/machine interface since the thermal properties are assumed equal.

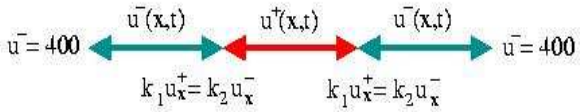


(a) 1D

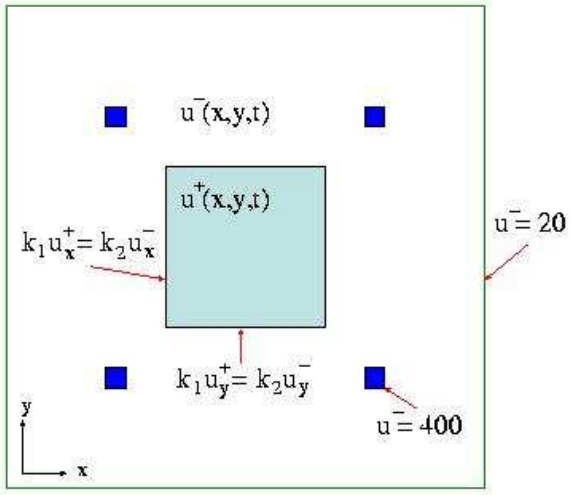


(b) 2D

Figure 1.3: 1D and 2D models with boundary conditions.

heat loss to air during opening is assumed to be small enough to be neglected in the first approximation. If the pouring time, which is rather short, is also ignored, a solution over a long time can be found by the following steps:

1. Start with initial temperature of 700°C inside the chamber and 30°C in the mould.
2. Solve the heat equation over 60 seconds.
3. Set the temperature in the chamber again to 700°C. This represents pouring in the liquid alloy for the next casting.
4. Go to 2.

During this process the temperature of the mould will heat up from 30°C to a stable temperature of about 400°C. This temperature will not be constant over time, but it will be the same at the beginning of each casting. So the temperature in the mould will "converge" to a periodic behaviour. Of interest is an understanding how fast this stable temperature is reached and how the time to reach it depends on different parameters, e.g. the position of the channels or a possible preheating of the mould.

## 1.3 A Fourier Method for the 1D Problem

In this section we apply a Fourier expansion in eigenfunctions to the one-dimensional problem to obtain some analytical estimates. The mathematical description of the one-dimensional problem can due to symmetry be given on half the domain with homogeneous Neumann boundary conditions at $x = 0$ and homogeneous Dirichlet boundary conditions at $x = L$ (by choosing a temperature scale which is 0 at the temperature of the channels of 400°C):

$$\begin{aligned}
u_t(x,t) &= D_1 u_{xx}(x,t) && \text{on } (0,d)\times(0,\infty) \\
u_t(x,t) &= D_2 u_{xx}(x,t) && \text{on } (d,L)\times(0,\infty) \\
u(x,0) &= u_0(x) && \forall x \in [0,L] \\
u_x(0,t) &= 0 && \forall t > 0 \\
u(L,t) &= 0 && \forall t > 0 \\
u^-(d,t) &= u^+(d,t) && \forall t > 0 \\
\kappa_1 u_x^-(d,t) &= \kappa_2 u_x^+(d,t) && \forall t > 0,
\end{aligned} \tag{1.6}$$

where

- $x$ is the distance from the symmetrical centre,
- $t$ is time,
- $u(x,t)$ is temperature,

- $d$ is the distance to from the centre to the edge of mould,
- $L$ is the distance to from the centre to the channels,
- $u_0(x)$ is the initial temperature distribution across the system,
- $D_1$ and $D_2$ are the diffusion constants of the two materials, and
- $\kappa_1$ and $\kappa_2$ are the heat conductivity constants of the two materials.

In order to obtain an analytical solution, we seek for solutions of the eigenvalue problem:

$$\begin{aligned} -D_1 u_1''(x) &= \lambda u(x) \quad \forall x \in (0,d) \\ -D_2 u_2''(x) &= \lambda u(x) \quad \forall x \in (d,L) \\ u'(0) &= 0 \\ u(L) &= 0 \\ u_1(d) &= u_2(d) \\ \kappa_1 u_1'(d) &= \kappa_2 u_2'(d). \end{aligned} \tag{1.7}$$

Each such function has a particular simple evolution under the heat equation

$$\begin{aligned} u_t(x,t) &= \lambda u(x,t) \\ u(x,0) &= u_0(x), \end{aligned} \tag{1.8}$$

which is just an ordinary differential equation. Its solution is

$$u(x,t) = e^{-\lambda t} u_0(x). \tag{1.9}$$

### Calculation of the Eigenfunctions

To obtain solutions to (1.7), we use the following ansatz with parameters $a$ and $b$:

$$\begin{aligned} u_1(x) &= \sin(b(L-d))\cos(ax) \\ u_2(x) &= \cos(ad)\sin(b(L-x)). \end{aligned} \tag{1.10}$$

This automatically guarantees continuity at $x = d$ as well as the correct boundary conditions at $x = 0$ and $x = L$. The second condition $\kappa_1 u_1'(d) = \kappa_2 u_2'(d)$ yields the relation

$$\tan(b(L-d))\tan(ad) = \frac{\kappa_2 b}{\kappa_1 a}, \tag{1.11}$$

and finally we employ the eigenvalue relation $-D(x)u''(x) = \lambda u(x)$, which yields

$$D_1 a^2 = \lambda = D_2 b^2. \tag{1.12}$$

Substituting $b = \sqrt{\frac{D_1}{D_2}}a$ into (1.11) yields a relation for $a$

$$\tan\left(\sqrt{\frac{D_1}{D_2}}a(L-d)\right)\tan(ad) = \frac{\kappa_2}{\kappa_1}\sqrt{\frac{D_1}{D_2}}, \tag{1.13}$$

which is fulfilled by a sequence of $(a_n)_{n\in\mathbb{N}}$, corresponding to a sequence of eigenfunctions and eigenvalues $\lambda_n = D_1 a_n^2$. Unfortunately equation (1.13) can not be solved analytically in any straight forward way, so the values $a_n$ have to be approximated numerically. This can be done up to machine accuracy by Newton iteration. Reasonable starting values can be found by a few bisection steps.
The first four eigenfunctions with the corresponding eigenvalues can be seen in Figures 1.4 to 1.7.

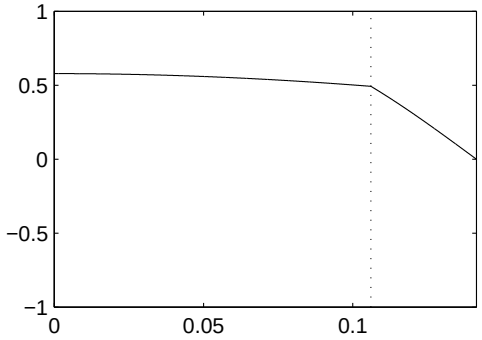


Figure 1.4: $\lambda_1 = 0.00256$

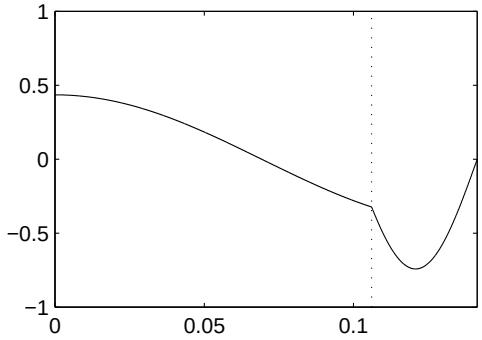


Figure 1.5: $\lambda_2 = 0.04855$

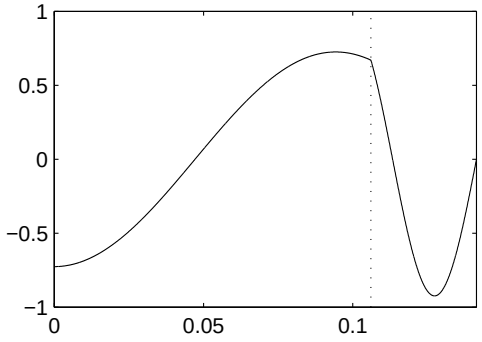


Figure 1.6: $\lambda_3 = 0.10479$

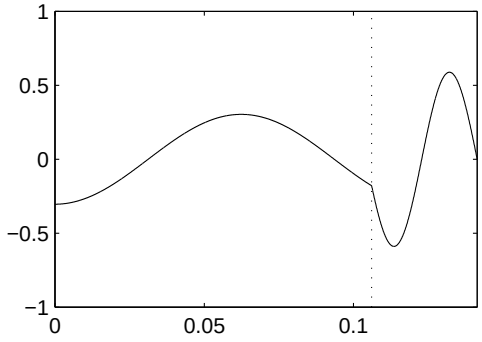


Figure 1.7: $\lambda_4 = 0.23930$

### Representation of Functions in the Fourier Basis

Omitting strict proofs for completeness we have found a basis of eigenfunctions of the subspace of $\mathbb{L}^2([0, L])$, which fulfils the boundary conditions at $x = 0$ and $x = L$ and continuity and slope conditions at $x = d$. Note that

the eigenfunctions will be linearly independent, but will in general not be orthogonal. While the operator $\kappa(x)\partial_{xx}$ is always self-adjoint, the operator $D(x)\partial_{xx}$ will only be self adjoint, if $\frac{\kappa_1}{\kappa_2} = \frac{D_1}{D_2}$.
Since this is in general not the case, the approximate representation of a function $u(x)$ on $[0, L]$ is not just obtained by

$$u(x) \approx \sum_{n=1}^{N} \frac{< u, u_n >}{< u_n, u_n >} u_n(x). \tag{1.14}$$

Instead we have to compute the Gramian

$$G = \begin{pmatrix} < u_1, u_1 > & \cdots & < u_1, u_N > \\ \vdots & \ddots & \vdots \\ < u_N, u_1 > & \cdots & < u_N, u_N > \end{pmatrix} \tag{1.15}$$

as well as the vector

$$b = \begin{pmatrix} < u, u_1 > \\ \vdots \\ < u, u_N > \end{pmatrix}. \tag{1.16}$$

The vector of Fourier coefficients is then obtained by

$$c = G^{-1} \cdot b, \tag{1.17}$$

i.e. we can approximate a function $u(x)$ by

$$u(x) \approx \sum_{n=1}^{N} c_n u_n(x). \tag{1.18}$$

Note that (1.18) becomes (1.14) for diagonal $G$, i.e. for the case $\frac{\kappa_1}{\kappa_2} = \frac{D_1}{D_2}$.

### The Method

The Fourier method for solving the original problem (1.6) will be the following:

1. Fix a number of Fourier coefficients $N$.

2. Calculate the parameters $a_1, \ldots, a_N$ for the first $N$ eigenfunctions as well as the eigenvalues $\lambda_1, \ldots, \lambda_N$.

3. Set up the Gramian $G$ and its compute its inverse.

4. Calculate the Fourier coefficients $c_1, \ldots, c_N$ of the initial temperature distribution $u_0$.

5. The solution at any time $t > 0$ will be

$$u(x) \approx \sum_{n=1}^{N} e^{-\lambda_n t} c_n u_n(x). \tag{1.19}$$

The main advantage of this method lies in the fact that once the Fourier coefficients are computed, we can calculate the result at any later time $t > 0$ directly, unlike finite difference methods, which have to go though the complete evolution in time.

### Applying the Method to the Original Problem

The initial condition in our problem is discontinuous at $x = d$, while all our eigenfunctions are continuous at $x = d$. We can still apply our method, but we will have to expect strong oscillations and slowly decaying Fourier coefficients. Luckily we are solving the heat equation, which lets high Fourier coefficients decay exponentially fast, so for $t$ not too small we will be close to the correct solution.
In Figures 1.8 to 1.11 the application of this method to our problem can be seen. Observe the oscillations for small times and the quality of the solution for larger times.

### Calculation of the Periodic Solution

Our original problem is governed by a quasi-periodic behaviour:

1. Set the function values on $[0, d]$ to a constant value $u_{alloy}$, keep function unchanged on $[d, L]$.
2. Apply the heat equation for a fixed time $t^*$.
3. Goto 1.

As we have pointed out in Section 1.2 this process will "converge" to a periodic behaviour. We can now use our Fourier method to approximate the function, which has the property that after applying steps 1. and 2. above to it, we obtain the same function again. In technical terms: We can obtain the stabilisation temperature directly.
The idea is to employ the fact that the diffusion constant at $[0, d]$ is larger than on $[d, L]$, and thus the temperature profile will be comparably flat on $[0, d]$. For the moment we assume it to be (nearly) constant. Then setting the function values on $[0, d]$ to a fixed value is just adding the function

$$h(x) = \begin{cases} 1 \text{ on } [0, d) \\ 0 \text{ on } [d, L] \end{cases} \tag{1.20}$$

Let now $c_n$ be the Fourier coefficients of our sought function and $\beta_n$ the Fourier coefficients of $h$. Then the steps above yield the following:

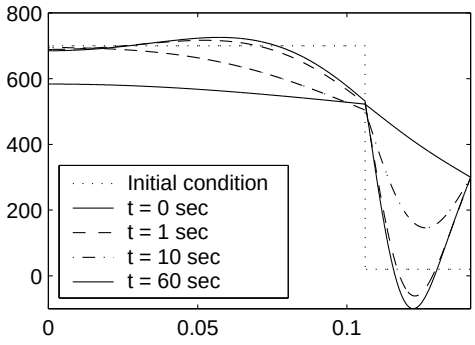


Figure 1.8: Using 5 eigenfunctions

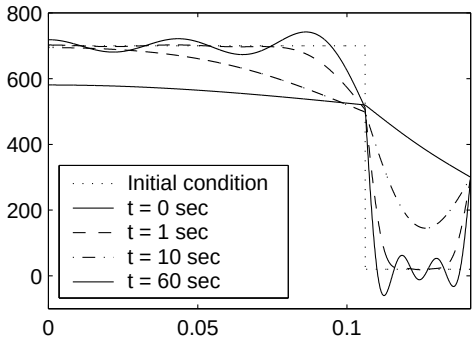


Figure 1.9: Using 10 eigenfunctions

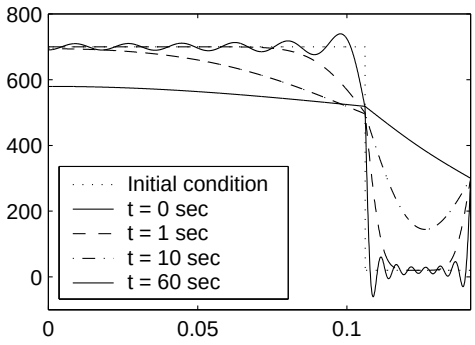


Figure 1.10: Using 25 eigenfunctions

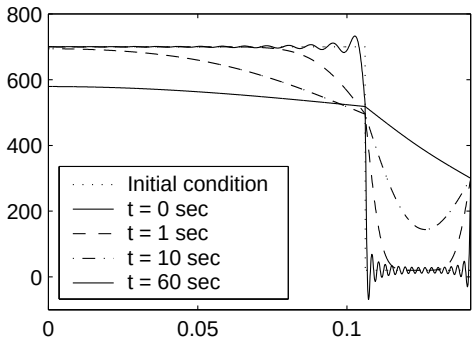


Figure 1.11: Using 60 eigenfunctions

1. $\tilde{c}_n = c_n + k \cdot \beta_n$, where $k \in \mathbb{R}$ is some constant
2. $c_n = e^{-\lambda_n t^*} \cdot \tilde{c}_n$.

Solving for $c_n$ yields

$$c_n = \frac{e^{-\lambda_n t^*}}{1 - e^{-\lambda_n t^*}} \cdot k \cdot \beta_n \tag{1.21}$$

The value of $k$ can be found by employing the fact that we know that after adding $h$ the value at $x = 0$ will be equal to $u_{alloy}$:

$$u_{alloy} = \sum_{n=1}^{N} (c_n + k\beta_n) u_n(0) = k \cdot \sum_{n=1}^{N} \frac{1}{1 - e^{-\lambda_n t^*}} \cdot \beta_n u_n(0) \tag{1.22}$$

This yields the following formula for Fourier coefficients of the stabilisation temperature:

$$c_n = \frac{u_{alloy}}{\sum_{n=1}^{N} \frac{1}{1-e^{-\lambda_n t^*}} \cdot \beta_n u_n(0)} \cdot \frac{e^{-\lambda_n t^*}}{1 - e^{-\lambda_n t^*}} \cdot \beta_n \tag{1.23}$$

In Figures 1.12 and 1.13 the results of this approximation are shown in comparison to the correct value obtained by a finite difference method with very small space and times steps. It can be seen that in spite of the fairly crude approximation to assume the temperature inside the alloy to be constant, the results are remarkably accurate.

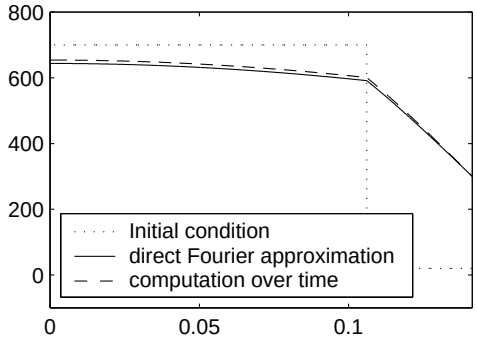


Figure 1.12: Direct Fourier method

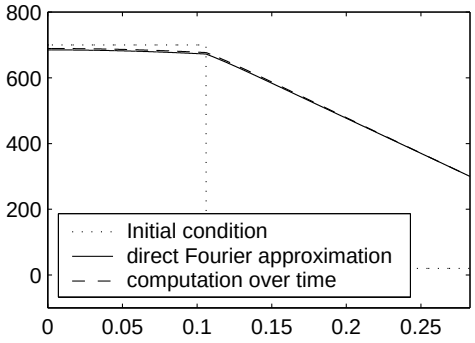


Figure 1.13: Another geometry

Note that this method allows to compute the stabilisation temperature directly, but does not give information about the time required to reach to this temperature. Here a formulation as a fixed point problem and estimation of the contraction constant could give answers.

### Conclusions

A Fourier expansion in eigenfunctions can be applied to the one-dimensional problem given in (1.6). As the results in this section show, the use of just 10 eigenfunctions gives accurate results, so the computational effort is significantly smaller compared to finite difference methods, which have to go through the whole evolution in time, while the Fourier method allows to compute the temperature distribution after 60 seconds directly. Additionally, the Fourier method allows to obtain results of interest, e.g. the stabilisation temperature, directly and thus very cheaply.
However, Fourier methods are limited to linear problems, i.e. they work well as long as the simple heat equation is being solved, but there is no straightforward way to include effects like a moving boundary as in considered Section 1.6. Here finite difference methods have to be used.

## 1.4 A Finite Difference Method for the 1D Problem

We would like to solve the 1D problem using finite differences to compare to the analytic solution presented above and the 2D FEMLAB finite element

numerics that follows. Also it is a first step before we can consider introducing a moving boundary to represent the solidification of the alloy within the mould.
From Section 1.2 the model is given by

$$\begin{aligned} u_t &= D_1 u_{xx} && \text{on} (0,d)\times(0,\infty), \\ u_t &= D_2 u_{xx} && \text{on} (d,L)\times(0,\infty), \\ u(x,0) &= u_0(x) && \forall x \in [0,L], \\ u_x(0,t) &= 0 && \forall t>0, \\ u(L,t) &= 400 && \forall t>0, \\ u^+(d,t) &= u^-(d,t) && \forall t>0, \\ \kappa_1 u_x^+(d,t) &= \kappa_2 u_x^-(d,t) && \forall t>0. \end{aligned} \tag{1.24}$$

The notations are the same as in Section 1.3, only the temperature scale is centred naturally around 0°C, not around 400°C, as it was necessary for the Fourier method.
We are to study the varying temperature as the mould is repeatedly used. Therefore before the mould is used at all we consider an initial condition $u_0(x)$ as

$$u_0(x) = \begin{cases} 700 & : \quad x \in [0,d] \\ 30 & : \quad x \in (d,L) \\ 400 & : \quad x = L \end{cases} \tag{1.25}$$

The high temperature for $x \in [0,d]$ represents the instant insertion of the hot alloy at $700°C$. The lower temperature $30°C$ for $x \in (d,L)$ represents the steel of the mould at room temperature. The $400°C$ is the temperature at the channels. When we wish to test the effect of repeated mouldings we can record the temperature of the mould at the end of one cycle and use it as the initial condition in the next.

### A First Order Explicit Method

First we need to define a grid of points in the $x$ and $t$ directions. For simplicity we define a grid so a line of points occurs on the boundary $x = d$ (see Figure 1.14). Then for a typical point P we can make the finite difference approximations

$$u_t(P) \approx \frac{u_{i,j+1} - u_{i,j}}{k}, \tag{1.26}$$

$$u_{xx}(P) \approx \frac{u_{i-1,j} - 2u_{i,j} + u_{i-1,j}}{h^2}, \tag{1.27}$$

where $h = x_{i,j} - x_{i-1,j}$, $k = x_{i,j} - x_{i,j-1}$. Substituting these expressions into our heat equation (1.24) yields the explicit finite difference method

$$u_{i,j+1} = r u_{i-1,j} + (1-2r) u_{i,j} + r u_{i+1,j}, \tag{1.28}$$

where

$$r := \frac{kD_m}{h^2}. \tag{1.29}$$

Here $D_m = D_1$ in the region $x < d$ and $D_m = D_2$ otherwise.

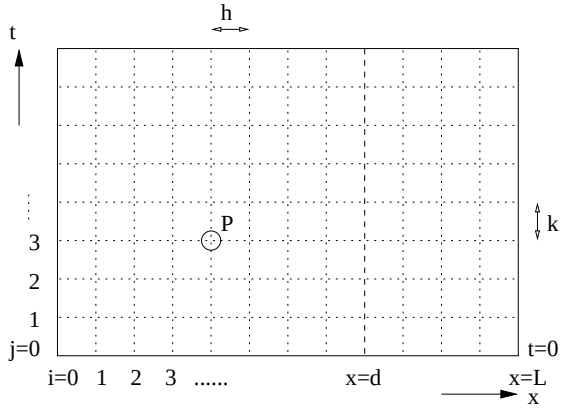


Figure 1.14: Grid layout for finite difference approximation in the 1D model

This defines how to find the points away from the boundary points. Now define the value of $i$ at which $x = d$ as $s$ and the total number of points to $x = L$ as $n$. On the boundary $x = 0$ we can guarantee homogeneous Neumann boundary conditions by assuming a fictitious point $x_{-1,j}$, which would equal $x_{1,j}$, and therefore

$$u_{xx}(0,t) \approx \frac{-2u_{0,j} + 2u_{1,j}}{h^2}, \tag{1.30}$$

We have assumed that the boundary at $x = d$ is nonsmooth, so we cannot define the second derivative across it. However using respectively backward and forward difference approximations for $u_x^-(d,t)$ and $u_x^+(d,t)$ we have

$$u_x^-(d,t) \approx \frac{u_{s,j} - u_{s-1,j}}{k} \tag{1.31}$$

$$u_x^+(d,t) \approx \frac{u_{s+1,j} - u_{s,j}}{k} \tag{1.32}$$

And so we can use the boundary conditions to find an expression for the value of $u(d,t)$ as

$$u_{s,j} = \frac{\kappa_2 u_{s+1,j} + \kappa_1 u_{s-1,j}}{\kappa_1 + \kappa_2} \tag{1.33}$$

The Dirichlet boundary condition at $x = L$ is straightforward to apply, i.e.

$$u_{n,j} = 400. \tag{1.34}$$

This completes the explicit method. Note that it has a CFL-condition

$$\frac{k}{h^2} < C, \tag{1.35}$$

as all explicit methods have for the heat equation, so for computations with an accurate resolution in $x$, an implicit method is required.

### A Second Order Implicit Method

For accurate computations explicit methods are restricted by the CFL-condition as stated before. We therefore set up a Crank-Nicolson method for our heat equation. It is second order accurate, unconditionally stable, and the conditions at the fixed ($x = d$) and moving boundary (see Section 1.6) apply very easily in this method.
From e.g. [5] we use the expression for the partial derivative $u_{xx}$ at the midpoint between six points on the grid as

$$u_{xx} \approx \frac{1}{h^2}(u_{i+1,j} - 2u_{i,j} + u_{i-1,j} + ui + 1, j + 1 - 2u_{i,j+1} + u_{i-1,j+1}). \tag{1.36}$$

The time derivative approximation remains the same

$$u_t \approx \frac{1}{k}(u_{i,j+1} - u_{i,j}) \tag{1.37}$$

Substituting these into the heat equation (1.24) gives the following expression for an interior point P

$$\begin{aligned} -ru_{i-1,j+1} + (2+2r)u_{i,j+1} - ru_{i+1,j+1} \\ = ru_{i-1,j} + (2-2r)u_{i,j} + ru_{i+1,j}, \end{aligned} \tag{1.38}$$

where

$$r := \frac{kD_m}{h^2}. \tag{1.39}$$

Here $D_m = D_1$ in the region $x < d$ and $D_m = D_2$ otherwise. The boundary condition at $x = 0$ and $x = L$ can be kept from the explicit case. The boundary condition at $x = d$ can be guranteed in an easier and more precise way, namely by the implicit relation

$$\kappa_1 u_{s+1,j+1} - (\kappa_1 + \kappa_2)u_{s+1,j} + \kappa_2 u_{s+1,j-1} = 0. \tag{1.40}$$

### Results and Conclusions

This simple finite difference case gave the same results as the Fourier expansion solution presented in Section 1.3. While it on the one hand provides a control for the results obtained previously, it will one the other hand be the basis for the more interesting problem of a moving boundary, considered in Section 1.6.

## 1.5 Solving the 2D Problem with FEMLAB

Although the one dimensional computations in Sections 1.3 and 1.4 gave insight into the qulitative behaviour of the solution, the particular values obtained were differing strongly from reality. Clearly the correct ratios between volumes and surfaces cannot be reflected in 1D models. The canonical step towards obtaining quantatively better results is going over to two-dimensional simulations. In this section we will use the finite element toolbox FEMLAB to compute solutions to the 2D problem.
Summarising Section 1.2, the 2D problem can be written as:

$$\begin{aligned}
u_t(x,y,t) &= D_1\nabla^2 u(x,y,t) && \text{on } \Omega_1 \times (0,\infty) \\
u_t(x,y,t) &= D_2\nabla^2 u(x,y,t) && \text{on } \Omega_2 \times (0,\infty) \\
u(x,y,0) &= u_0(x,y) && \text{on } \Omega_1 \cup \Omega_2 \\
u(x,y,t)\big|_{\Gamma_C} &= T_c && \forall t > 0 \\
u(x,y,t)\big|_{\Gamma_A} &= T_a && \forall t > 0 \\
u(x,y,t)\big|_{\Gamma_M^+} &= u(x,y,t)\big|_{\Gamma_M^-} && \forall t > 0 \\
\kappa_1\nabla u(x,y,t)\big|_{\Gamma_M^+} &= \kappa_2\nabla u(x,y,t)\big|_{\Gamma_M^-} && \forall t > 0,
\end{aligned} \tag{1.41}$$

where $\Gamma_C$ is the channel/mould interface, $\Gamma_A$ is the machine/air interface, $\Gamma_M$ is the mould/alloy interface, $T_c$ is the channel temperature and $T_a$ is the room temperature.
To solve the above model the FEMLAB program was used. FEMLAB is finite element toolbox built on top of MATLAB, and can be used to solve a wide variety of engineering problems with little programming effort. For the current problem the element method is particularly well suited because the flux continuity condition (the last equality of equation (1.41)) will be fulfilled simply by virtue of the domain decomposition. This is easily seen from the weak formulation. The rest of the conditions, i.e. the Dirichlet boundary conditions and the initial conditions are easily specified through the program interface.
Simple scripting allows for simulation of the casting process, and some examples of graphical FEMLAB output are shown in Figures 1.15 and 1.16 (a)-(d). In all computations the FEMLAB defaults were used, i.e. second order Lagrange elements in combination with the very general MATLAB function *ode15s* for the time evolution.

### Position of Channels

With a working 2D model some of the questions posed in the introduction can be answered. Figure 1.17 shows a plot of the temperature stabilisation time, measured in number of castings required for stabilisation, as a function of the diagonal distance between the mould chamber and the alloy. The

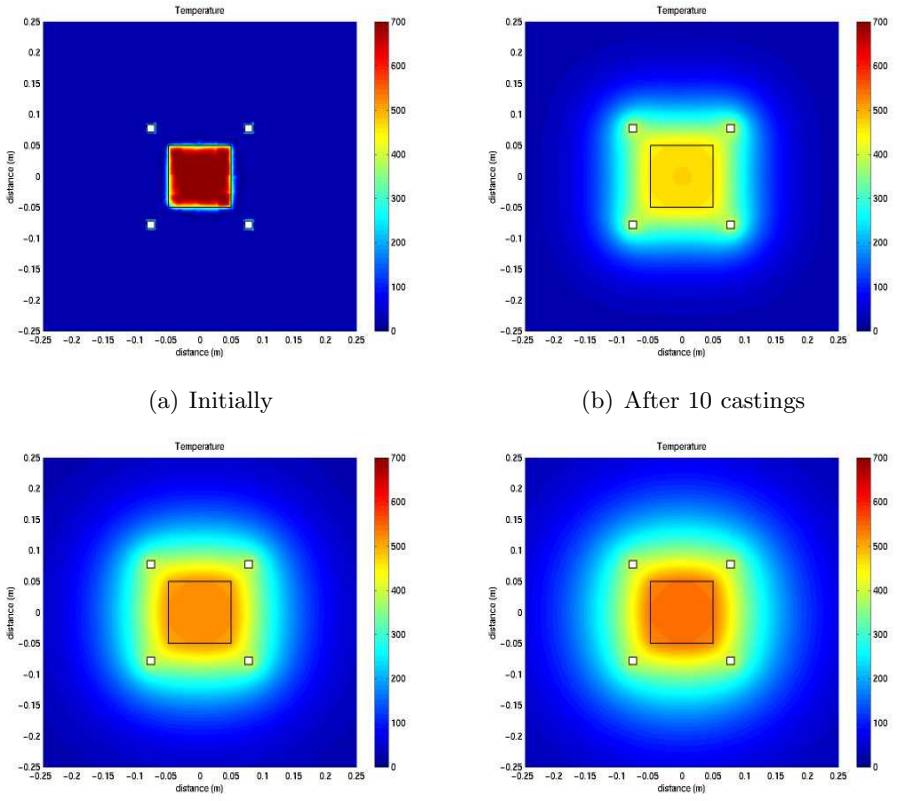


(a) Initially

(b) After 10 castings

(c) After 20 castings

(d) After 30 castings

Figure 1.15: Solution of the 2D model with FEMLAB

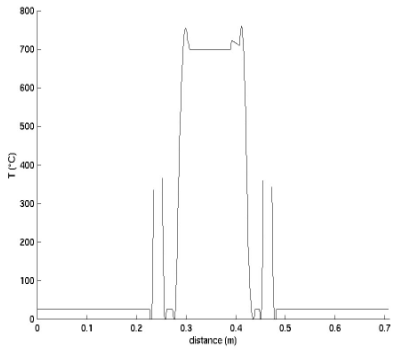


(a) Initially

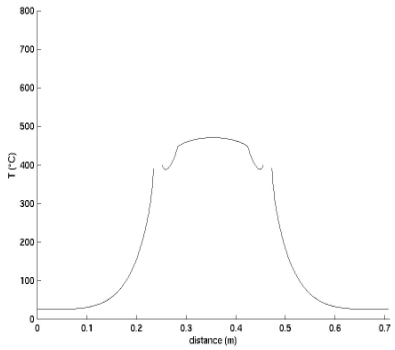


(b) After 10 castings

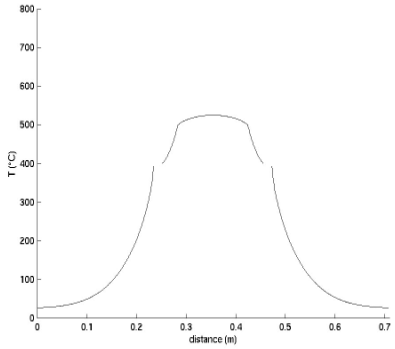


(c) After 20 castings

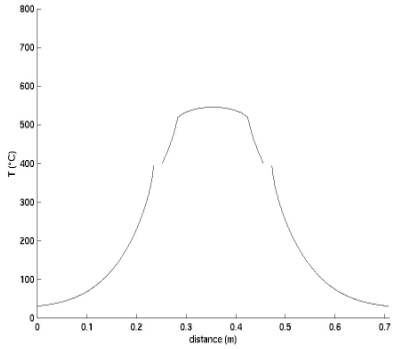


(d) After 30 castings

Figure 1.16: Values along the diagonal of the solution shown in Figure 1.15

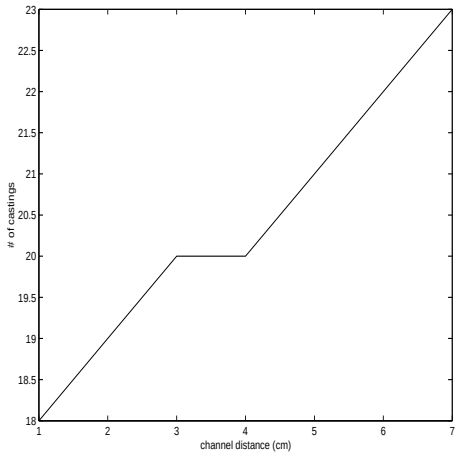


Figure 1.17: Temperature stabilisation time vs. channel distance.

temperature was considered as stable when the average difference between two subsequent mould temperature distributions was below a given constant. Expectedly, the stabilisation time decreases with decreasing distance, so the conclusion is that the channels should be placed as close to the chamber as possible. Of more interest is the fact that the stable temperature only varied between 511°C and 544°C. This implies that the channels in fact have little effect on the stable temperature, meaning that production temperature might be reached even without the channels, although this would of course take much longer.

### Preheating

An alternative to starting the casting immediately is preheating the mould by letting the hot fluid run through the channels for a certain amount of time. Figure 1.18 shows the stabilisation time, measured in number of subsequent castings required for stabilisation, as a function of preheating times in the range 0-30 minutes.

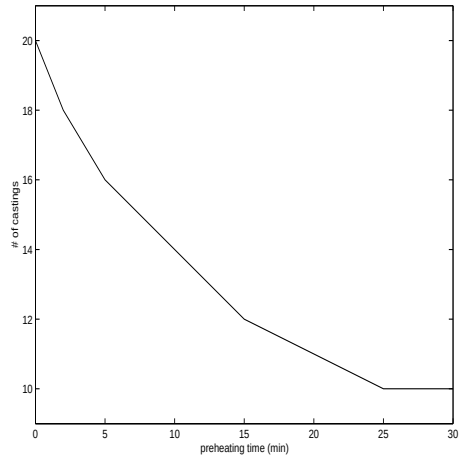


Figure 1.18: Stabilisation time vs. preheating time.

After only 20 minutes of preheating there is a reduction of almost 50% in the required number of castings, so preheating might certainly be worthwhile. When having information about the relative costs involved for preheating and rejecting low-quality products, it is very likely to find an optimal, i.e. cost-efficient, preheating time.

## 1.6 The 1D Problem with Change of State

So far we have ignored the change of state of the alloy during the casting process. But in fact the alloy in inserted in the liquid state, and is solid

when being taken out (at least almost completely). In this section we will include the state transition into the one-dimensional problem, to answer the question, if it makes a relevant difference to consider or neglect the change of state.
Due to the temperature gradient the alloy will start solidifying at the outside (at $x = d$), once the temperature has reached the melting temperature of about $500°C$. So we will have a boundary between solid and liquid state, which will move to the interior (toward $x = 0$). Considering this effect will change the results for the following reasons:

- The conductivities and diffusion constants are different for liquid and solid alloy.
- When solidifying, the latent energy of liquid alloy will be released.

The cooling process will consist of three steps:

1. All alloy is liquid.
2. The alloy is solid at $x = d$ and liquid at $x = 0$. Somewhere in between a boundary moves toward $x = 0$.
3. All alloy is solid.

Steps 1. and 3. can be computed as presented in previous sections. Step 2. however requires a description of the moving boundary, physically and in our finite difference scheme.

### The Stefan Condition

Let $s(t)$ be the position of the boundary between liquid and solid state. The large diffusion constant in the liquid alloy and the fact that one will have a temperature increase at the boundary due to the release of latent heat give rise to the approximation that the temperature in the liquid alloy ($x \in [0, s(t)]$) is constant at the melting temperature of the alloy. In the solid alloy ($x \in [s(t), d]$) as well as in the mould ($x \in [d, L]$) there will be a temperature profile with the condition for the slopes at $x = d$. Note that now the conductivity and diffusion constant for solid alloy have to be used. The observation that the latent heat released must be equal to the heat conducted back through the point $x = s(t)$ yields a condition for the speed of the boundary, which is known as the *Stefan condition* [3]:

$$\dot{s}(t) = \frac{k}{\lambda\rho} \cdot u_x(s(t), t) \tag{1.42}$$

Here $k$ is the conductivity and $\rho$ the density of the solid alloy, and $\lambda$ is the latent heat coefficient of the alloy.

### Finite Difference Scheme with Moving Boundary

We include the moving boundary between liquid and solid alloy into our finite difference method by an operator splitting approach. We take an equidistant grid with mesh size $h$, which is aligned with the boundary between solid alloy and the mould ($x = d$). The position of the moving boundary $s(t)$ is saved as a floating point number. In each time step we compute the following:

1. Approximate $u_x(s(t), t)$ by finite differences and change $s(t)$ according to (1.42).

2. Evolve the heat equation with time step $\Delta t$. Here $s(t)$ is included as an additional grid point.

Figure 1.19 shows the finite difference method with the boundary included as an additional point. The distance between $s(t)$ and the next grid point in the solid phase is denoted by $h_2$.

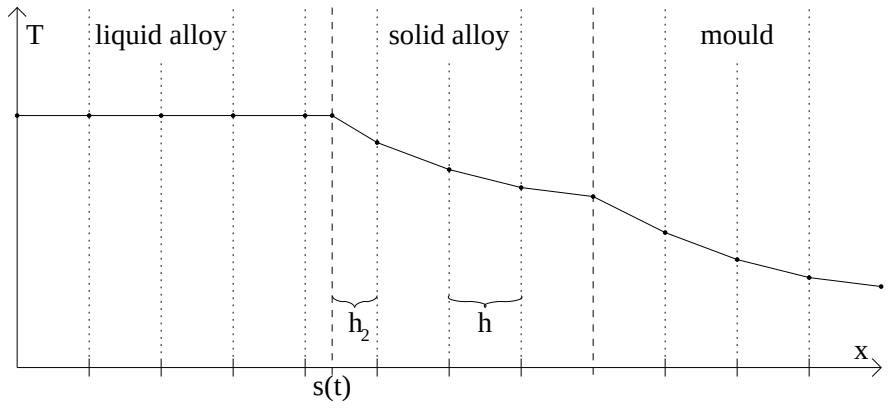


Figure 1.19: Finite Difference Scheme with Moving Boundary

The two steps are implemented in the following way:

1. Let $u_{melt}$ denote the melting temperature of the alloy and $u_j$ the temperature at the next grid point. The temperature gradient at the moving boundary $u_x(s)$ could be approximated by

$$u_x(s) \approx \frac{u_j - u_{melt}}{h_2}, \tag{1.43}$$

but this causes numerical instabilities once $h_2$ becomes small, which can happen if the moving boundary can fall close to a grid point. We thus use the stable approximation

$$u_x(s) \approx \frac{u_{j+1} - u_{melt}}{h + h_2}. \tag{1.44}$$

This yields the new position of the boundary to be

$$s(t+\Delta t) = s(t) + \Delta t \frac{k}{\lambda \rho} \cdot \frac{u_{j+1} - u_{melt}}{h + h_2}. \tag{1.45}$$

2. As in the Section 1.4 we use the Crank-Nicolson method for the heat equation, and include the moving boundary as an additional grid point. Since the temperature at the boundary and at all grid points left of it is constant at the melting temperature of the alloy, no computation has to be done here. For simplicity we keep these points in our computation. For all points right of the moving boundary besides the first one, the matrices stay unchanged, too. Only for the first grid point right to the moving boundary we have to modify the matrices. Let the boundary be grid point $j-1$, the point of our interest be grid point $j$, and the point right to it grid point $j+1$. Since in general $h_2 < h$, we have to approximate $u_{xx}$ at this point by

$$\begin{aligned} u_{xx} &\approx \frac{\frac{u_{j+1}-u_j}{h} - \frac{u_j - u_{j-1}}{h_2}}{\frac{1}{2}(h+h_2)} = \frac{h_2 u_{j+1} - (h_2+h)u_j + h u_{j-1}}{\frac{h+h_2}{2} h h_2} \\ &= \frac{2}{h(h+h_2)} \cdot u_{j+1} - \frac{2}{h h_2} \cdot u_j + \frac{2}{h_2(h+h_2)} \cdot u_{j-1}. \end{aligned} \tag{1.46}$$

This yields the following finite difference approximation around the point $j$:

$$\begin{aligned} &-\frac{\Delta t D}{h(h+h_2)} \cdot u_{j+1}^{n+1} + (1 + \frac{\Delta t D}{h h_2}) \cdot u_j^{n+1} - \frac{\Delta t D}{h_2(h+h_2)} \cdot u_{j-1}^{n+1} \\ &= \frac{\Delta t D}{h(h+h_2)} \cdot u_{j+1}^{n} + (1 - \frac{\Delta t D}{h h_2}) \cdot u_j^{n} + \frac{\Delta t D}{h_2(h+h_2)} \cdot u_{j-1}^{n}. \end{aligned} \tag{1.47}$$

This yields the following scheme for the evolution of one time step with the heat equation:

$$A u^{n+1} = B u^n, \tag{1.48}$$

where

$$A = \begin{pmatrix} 1 & 0 & 0 & 0 & 0 & 0 & 0 \\ 0 & 1 & 0 & 0 & 0 & 0 & 0 \\ 0 & -\frac{\Delta t D_1}{h_2(h+h_2)} & 1 + \frac{\Delta t D_1}{h h_2} & -\frac{\Delta t D_1}{h(h+h_2)} & 0 & 0 & 0 \\ 0 & 0 & -\frac{\Delta t D_1}{2h^2} & 1 + \frac{\Delta t D_1}{h^2} & -\frac{\Delta t D_1}{2h^2} & 0 & 0 \\ 0 & 0 & 0 & -\kappa_1 & \kappa_1 + \kappa_2 & -\kappa_2 & 0 \\ 0 & 0 & 0 & 0 & -\frac{\Delta t D_2}{2h^2} & 1 + \frac{\Delta t D_2}{h^2} & -\frac{\Delta t D_2}{2h^2} \\ 0 & 0 & 0 & 0 & 0 & -\frac{\Delta t D_2}{2h^2} & 1 + \frac{\Delta t D_2}{h^2} \end{pmatrix} \tag{1.49}$$

and

$$B = \begin{pmatrix} 1 & 0 & 0 & 0 & 0 & 0 & 0 \\ 0 & 1 & 0 & 0 & 0 & 0 & 0 \\ 0 & \frac{\Delta t D_1}{h_2(h+h_2)} & 1 - \frac{\Delta t D_1}{h h_2} & \frac{\Delta t D_1}{h(h+h_2)} & 0 & 0 & 0 \\ 0 & 0 & \frac{\Delta t D_1}{2h^2} & 1 - \frac{\Delta t D_1}{h^2} & \frac{\Delta t D_1}{2h^2} & 0 & 0 \\ 0 & 0 & 0 & 0 & 0 & 0 & 0 \\ 0 & 0 & 0 & 0 & \frac{\Delta t D_2}{2h^2} & 1 - \frac{\Delta t D_2}{h^2} & \frac{\Delta t D_2}{2h^2} \\ 0 & 0 & 0 & 0 & 0 & \frac{\Delta t D_2}{2h^2} & 1 - \frac{\Delta t D_2}{h^2} \end{pmatrix}. \tag{1.50}$$

The above matrices represent the structure:

- The first two lines correspond to the liquid alloy, which stays at the constant melting temperature. They stand for possibly large block identity matrices.
- The third lines correspond to the first point next to the moving boundary.
- The fourth line again represents possibly large tridiagonal matrices corresponding to the solid alloy. $D_1$ is the diffusion constant for solid alloy.
- The fifth lines guarantee the slope condition at the boundary between solid alloy and mould to be satisfied. $\kappa_1$ is the conductivity of solid alloy, and $\kappa_2$ is the conductivity of the mould.
- The sixth and seventh lines stands again for tridiagonal matrices belonging to the mould. $D_2$ is the diffusion constant of the mould. The last line guarantees homogeneous Dirichlet boundary conditions.

### The Complete Cooling Process

As stated previously, the cooling process consists of three steps, which we have treated separately so far. Note that the assumption of the liquid alloy to have constant temperature when a moving boundary is existent, is only approximately correct. As could be seen in previous sections, there *is* a temperature gradient in the alloy, although not as large as the gradient in the mould. This means, we have to define when the first step ends, i.e. when the melting temperature is reached. We chose this condition to be that the average temperature over the whole alloy becomes less than the melting temperature. One can see in the numerical results below, that the temperature will have a small discontinuity in time due to this effect.
The transfer from the second to the third step, however, is not a problem. Once the moving boundary has reached $x = 0$, we go over to a first finite difference scheme without a moving boundary again, only with solid instead of liquid alloy.

### Numerical Results

Figures 1.20 to 1.25 show the cooling process over a long time, without removing the product. The computation with the moving boundary between solid and liquid alloy is plotted in comparison to a computation where the heat equation without a moving boundary is being solved over the whole time, once using the conductivities and diffusion constants of liquid alloy, and once using the appropriate constants for solid alloy.
One can observe that the latent energy plays an important role, since the computation with moving boundary show a significantly slower cooling as both other computation. If one wants accurate results, the latent energy must not be neglected. Furthermore it has to be pointed out that the one-dimensional computation reflects the qualitative behaviour, but does not give quantitatively correct results. As one can see in Figure 1.22, after 60 seconds the material is still half liquid, although the mould is at room temperature in the beginning.

## 1.7 Conclusions and Outlook

The Fourier coefficient method for the 1D problem described in Section 1.3 provides a way of gaining insight into the solution's behaviour with little computational effort. Particularly handy is the possibility of directly computing the stabilisation temperature. For the model considering the state transition, however, the Fourier method cannot be used. The moving boundary between liquid and solid state can be included into the finite difference method, as shown in Section 1.6.
Solving the 2D problem with FEMLAB is naturally much more computationally intensive, but the results are also more informative, and should be closer to reality. The simulations clearly show that the channels should be placed as close to the chamber as possible, and that preheating the mould might be a good idea if the associated cost is not too great.
However, as seen in Section 1.6, ignoring the change of state is an over-simplification of the problem. A natural next step would therefore be to extend the 2D model to also include the moving boundary between liquid and solid state. Since in 2D the geometry of the moving boundary becomes non-trivial, including the state transition into a FEMLAB or finite difference simlulation is by no means a trivial task. Furthermore, in both 1D and 2D the effect of neglecting the heat loss during the opening of the mould should be investigated for more precise results.
Although the 1D and 2D models show *indications* of what might happen in different situations and represent the qualitative behaviour well, only a complete 3D simulation can hope to accurately approximate the true solution, especially if one wants to consider the real geometry of the mould.
The preferred option to obtain quantitative results should be a 3D simulation

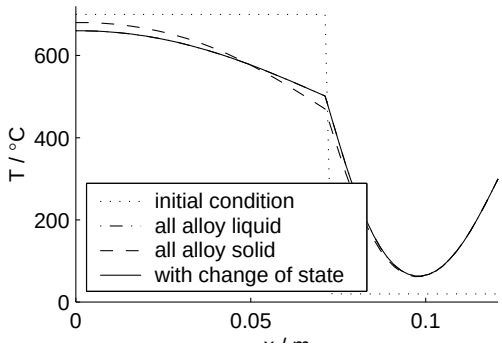


Figure 1.20: Liquid alloy ($t = 10$s)

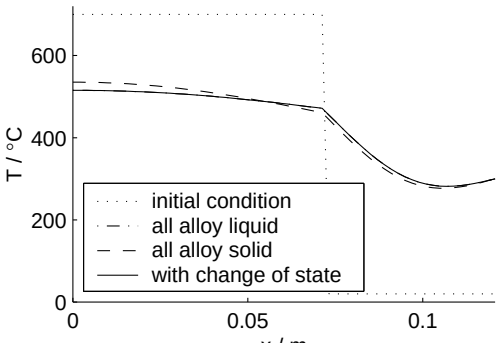


Figure 1.21: Solidification ($t = 48$s)

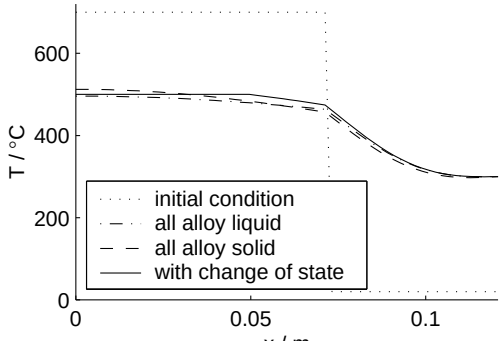


Figure 1.22: $b = 5.5$cm ($t = 60$s)

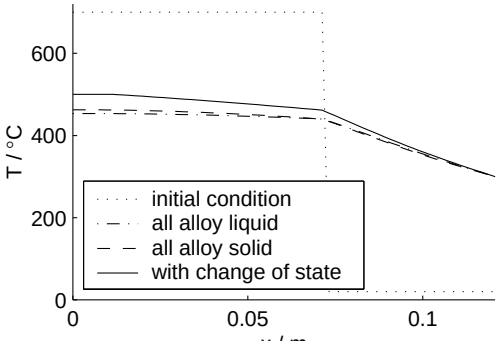


Figure 1.23: $b = 2$cm ($t = 110$s)

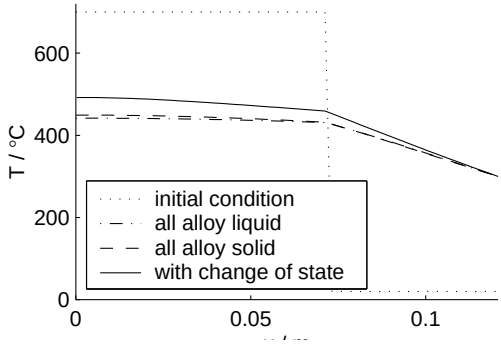


Figure 1.24: All solidified ($t = 135$s)

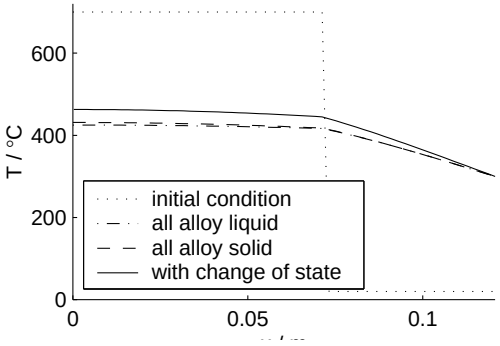


Figure 1.25: Solid alloy ($t = 180$s)

with a simplified geometry, where the state transition is described in a mostly simple way. Since 3D simulations with FEMLAB are memory intensive, for a simple geometry coding a numerical method by hand might be the best option.

# Bibliography


[1] J. R. Cannon, "The one-dimensional heat equation", Addison-Wesley Publishing Company, Reading (1984).

[2] N. D. Fowkes, J. J. Mahony, "An introduction to mathematical modelling", John Wiley and Sons, New York (1994).

[3] R. G. Fulford, P. Broadbridge, "Industrial Mathematics. Case studies in the diffusion of heat and matter", Cambridge University Press (2001).

[4] C. C. Lin, L. A. Segal, "Mathematics applied to deterministic problems in the natural sciences", SIAM New York (1988).

[5] H. R. Schwarz, "Numerical Analysis, A Comprehensive Introduction", John Wiley and Sons (1989).